Synthesis, Structural Characterization, and Computational Studies of Novel Diiodine Adducts with the Heterocyclic Thioamides N-Methylbenzothiazole-2-thione and Benzimidazole-2-thione: Implications with the Mechanism of Action of Antithyroid Drugs

Ghada J. Corban,[†] Sotiris K. Hadjikakou,*,[†] Nick Hadjiliadis,*,[†] Maciej Kubicki,[‡] Edward R. T. Tiekink,[§] Ian S. Butler,[||] Evangelos Drougas,[⊥] and Agnie M. Kosmas[⊥]

Section of Inorganic and Analytical Chemistry, Department of Chemistry, University of Ioannina, 45150 Ioannina, Greece, Department of Chemistry, A. Mickiewicz University, ul. Grunwaldzka 6, 60-780 Poznan, Poland, Department of Chemistry, The University of Texas at San Antonio, San Antonio, Texas 78249-0698, Department of Chemistry, McGill University, 801 Sherbrooke, Montreal, Quebec, Canada H2A 2K6, and Section of Physical Chemistry, Department of Chemistry, University of Ioannina, 45150 Ioannina, Greece

Reaction of N-methylbenzothiazole-2-thione ($C_8H_7NS_2$ or NMBZT) with diiodine produced the charge-transfer (ct) complex [(NMBZT)·I_2] (**1**). NMBZT reacts with diiodine in the presence of $FeCl_3$ in a molar ratio of 3:6:1 and forms the ionic complex {[(NMBZT)$_2$I]$^+$·[FeCl$_4$]$^-$} (**2**) together with {[(NMBZT)$_2$I]$^+$·[I$_7$]$^-$} (**2a**) iodonium salt. The reaction of benzimidazole-2-thione ($C_7H_6N_2S$ or MBZIM) with diiodine on the other hand results in the formation of the ct {[(MBZIM)$_2$I]$^+$[I$_3$]$^-$}·[(MBZIM)·I_2] (**3**) compound. The compounds have been characterized by elemental analyses, DTA-TG, FT-Raman, FT-IR, UV–vis, and ^{1}H NMR spectroscopies, and X-ray crystal structure determinations. Compound **1**, $C_8H_7I_2NS_2$, is orthorhombic with a space group Pna2$_1$ and a = 12.5147(13) Å, b = 22.536(3) Å, c = 4.2994(5) Å, and Z = 4. Compound **2**, $C_{16}H_{14}Cl_4FeIN_2S_4$, is monoclinic, space group C2/c, a = 35.781(2) Å, b = 7.4761(5) Å, c = 18.4677(12) Å, β = 107.219(1)°, and Z = 8. Compound **3**, $C_{21}H_{18}I_6N_6S_3$, monoclinic, space group P2$_1$/n, a = 14.0652(11) Å, b = 22.536(3) Å, c = 4.2994(5) Å, β = 99.635(7)°, and Z = 4, consists of two component moieties cocrystallized, one neutral which contains the benzimidazole-2-thione (MBZIM) ligand bonded with an iodine atom through sulfur, forming a compound with a "spoke" structure [(MBZIM)I$_2$] **3a**, while the other is the ionic complex {[(MBZII)$_2$I]$^+$·[I$_3$]$^-$} (**3b**). The X-ray crystal structure of **1** shows a bond between the thione-sulfur atom and one of the iodine atoms in an essentially planar arrangement. In the cation of **2**, an iodine is coordinated by two thione-sulfur atoms in a linear arrangement but the molecule is not planar. For the first time in the solid state a spoke–ionic mixed complex has been characterized in **3**. One component of the structure is a molecular diiodine adduct, i.e., [(MBZIM)I$_2$] (**3a**), with a linear coordination geometry in a decidedly planar arrangement, and the other component is an ionic adduct {[(MBZIM)$_2$I]$^+$·[I$_3$]$^-$} (**3b**) with the cation having an arrangement similar to that found for **1**. Theoretical calculations using density functional (DFT) and ab initio Hartree–Fock theory have been carried out for **1** and **3a,b**. The results are consistent with the experimental data. Conclusions on the behavior of a thioamide, when used as an antithyroid drug, have also been made.

Introduction

The perturbation of the I–I bond when diiodine interacts with heterocycles such as thiones leads to novel complexes containing iodine.[1–10] Various types of such complexes have been obtained thus far, including charge transfer (ct) with the so-called "spoke" or "extended spoke" structures (DS·I_2 or DS·I_2···I_2),[1a–c,2,3a,4b,5a,b,d,6a,b,7b–d,8a,b] the "T-shape" structure,[2]

* To whom correspondence should be addressed. E-mail: nhadjis@cc.uoi.gr (N.H.); shadjika@cc.uoi.gr (S.K.H.). Fax: 30-26510-44831.
† Section of Inorganic and Analytical Chemistry, University of Ioannina.
‡ Department of Chemistry, A. Mickiewicz University.
§ Department of Chemistry, The University of Texas at San Antonio.
|| Department of Chemistry, McGill University.
⊥ Section of Physical Chemistry, Department of Chemistry, University of Ioannina.

iodine(I) coordinated to two thioamides to form "iodonium salts" ([DS−I−DS]$^+$•(I$_3$)$^-$),[1a,2,4b,7a,9b,c] oxidation products of formula DS−I,[8a] dications of formula [DS]$_2$(I$_n^-$)$_2$,[4a,5e,9a] and monocations of formula [DS−SDH](I$_3$)$^-$.[1d,4a]

The interest in the study of structure−activity relationship of thioamides against diiodine is stimulated by the interest in the molecular compounds formed between antithyroid drugs and diiodine,[1,11−13] since thioamides are known to exhibit antithyroid activity.[13] The most commonly employed antithyroid drugs in use are 6-*n*-propylthiouracil (PTU), *N*-methylimidazoline-2-thione (methimazole, MMI), and 3-methyl-2-thioxo-4-imidazoline-1-carboxylate (carbimazole) (CBZ).[13] 1,3-Bis(hydroxymethyl)benzimidazoline-2-thione has also been used[13] for this purpose. Thyroid-peroxidase (TPO), an iron−porphyrin enzyme,[14,15] is responsible for the oxidation of iodide anions to active diiodine.[15,16] The proposed reaction scheme for the mechanism of action of TPO involves the formation of the {[TPO−OI]$^-$} intermediate complex which reacts with tyrosine to give mono- and diiodotyrosine and TPO.[15] It has been shown that MMI[4a] is readily oxidized by the thyroid-peroxidase (TPO) to form MMI disulfide (bis[1-methylimidazole(2)] disulfide), while activated iodine is reduced to iodide anion simultaneously. We also recently demonstrated that PTU forms weak charge-transfer complexes (ct) with diiodine.[1c] Thiazolidine-2-thione (TZDTH), an antithyroid agent,[13] formed a double coordinated iodine(I) complex of formula [{(tzdtH)$_2$I$^+$}•I$_3^-$•2I$_2$][1a] when reacted with excess diiodine. Although it has been proposed[1,11−12] that thioamides inhibit the formation of thyroid hormones by depressing the incorporation of oxidized iodides to tyrosine, a precursor of the T3 and T4 hormones, the precise mechanism of this trapping is still a matter of further investigation.

In this paper, we report the structural and spectroscopic characterization of two new diiodine complexes with the heterocyclic thioamides *N*-methylbenzothiazole-2-thione (C$_8$H$_7$NS$_2$ or NMBZT, **I**) and benzimidazole-2-thione (C$_7$H$_6$N$_2$S or MBZ1M, **II**) of formulas {[(NMBZT)$_2$I]$^+$•[FeCl$_4$]$^-$} (**2**) and {[(MBZIM)$_2$I]$^+$•[I$_3$]$^-$}•[(MBZIM)I$_2$] (**3**). The crystal structure of [(NMBZT)•I$_2$] (**1**), compound previously isolated as a powder,[6b] is also reported. On the basis of the experimental data and theoretical calculations, an attempt to correlate the results with the mechanism of action of antithyroid drugs is made.
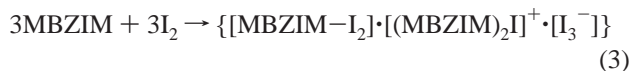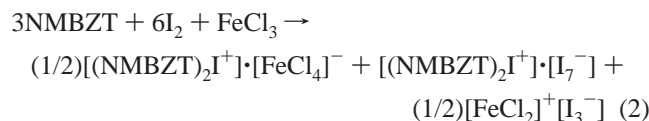

(I)   (II)
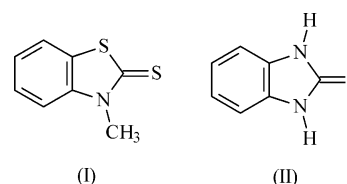
Results and Discussion

Reactions. NMBZT (**I**) reacts with I$_2$ in a molar ratio of 1:1 to form the neutral adduct [(NMBZT)•I$_2$] (**1**) (eq 1). When it reacts with diiodine in the presence of FeCl$_3$ in a molar ratio of 3:6:1 (NMBZT:I$_2$:FeCl$_3$), complex {[(NMBZT)$_2$I]$^+$}•[FeCl$_4$]$^-$ (**2**) together with {[(NMBZT)$_2$I$^+$}• [I$_7$]$^-$ (**2a**) (eq 2) is formed. MBZIM (**II**), on the other hand, reacts with I$_2$ in a molar ratio of 1:1 to form the mixed neutral and ionic compound {[(MBZ1M)$_2$I]$^+$}•[I$_3$]$^-$}•[(MBZIM)I$_2$]•**3** (eq 3).

(1) (a) Daga, V.; Hadjikakou, S. K.; Hadjiliadis, N.; Kubicki, M.; dos Santos, J H. Z.; Butler, I. S. *Eur. J. Inorg. Chem* **2002**, 1718−1728. (b) dos Santos, J H. Z.; Butler, I. S.; Daga, V.; Hadjikakou, S. K.; Hadjiliadis, N. *Spectrochim. Acta, Part A* **2002**, *58*, 2725−2735. (c) Antoniadis, C. D.; Corban, G.; Hadjikakou, S. K.; Hadjiliadis, N.; Kubicki, M.; Warner, S.; Butler, I. S. *Eur. J. Inorg Chem* **2003**, 1635−1640. (d) Antoniadis, C. D.; Hadjikakou, S. K.; Hadjiliadis, N.; Kubicki, M.; Butler, I. S. *Eur. J. Inorg. Chem.* **2004**, 4324−4329.
(2) Boyle, P. D.; Godfrey, S. M. *Coord. Chem. Rev.* **2001**, *223*, 265−299.
(3) (a) Deplano, P.; Ferraro, J. R.; Mercuri, M. L.; Trogu, E. F. *Coord. Chem. Rev.* **1999**, *188*, 71−95. (b) Aragoni, M. C.; Arca, M.; Devillanova, F. A.; Garau, A.; Isaia, F.; Lippolis, V.; Verani, G. *Coord. Chem. Rev.* **1999**, *184*, 271−290.
(4) (a) Aragoni, M. C.; Arca, M.; Demartin, F.; Devillanova, F. A.; Garau, A.; Isaia, F.; Lippolis, V.; Verani, G. *J Am. Chem. Soc.* **2002**, *124*, 4538−4539. (b) Boyle, P. D.; Christie, J.; Dyer, T.; Godfrey, S. M.; Howson, I. R.; McArthur, C.; Omar, B.; Pritchard, R. G.; Williams, G. R. *J. Chem. Soc., Dalton Trans.* **2000**, 3106−3112. (c) Esseffar, M.; Bouab, W.; Lamsabhi, A.; Abboud, J. L. M.; Notario, R.; Yanez, M. *J. Am. Chem. Soc.* **2000**, *122*, 2300−2308.
(5) (a) Bigoli, F.; Deplano, P.; Ienco, A.; Mealli, C.; Mercuri, M. L.; Pellinghelli, M. A.; Pintus, G.; Saba, G.; Trogu, E. F. *Inorg. Chem.* **1999**, *38*, 4626−4636. (b) Bricklebank, N.; Skabara, P. J.; Hibbs, D. E.; Hursthouse, M. B.; Malik, K. M. A. *J. Chem. Soc., Dalton Trans.* **1999**, 3007−3014. (c) Demartin, F.; Devillanova, F. A.; Garau, A.; Isaia, F.; Lippolis, V.; Verani, G. *Polyhedron* **1999**, *18*, 3107−3113. (d) Apperley, D. C.; Bricklebank, N.; Burns, S. L.; Hibbs, D. E.; Hursthouse, M. B.; Malik, K. M. A. *J. Chem. Soc., Dalton Trans.* **1998**, 1289−1292. (e) Bigoli, F.; Deplano, P.; Mercuri, M.; Pellinghelli, M.; Pintus, G.; Trogu, E. F.; Zonnedda, G.; Wang, H. H.; Williams, J. M. *Inorg. Chim. Acta* **1998**, *273*, 175−183.
(6) (a) Bigoli, F.; Deplano, P.; Mercuri, M. L.; Pellinghelli, M. A.; Sabatini, A.; Trogu, E. F.; Vacca, A. *J. Chem. Soc., Dalton Trans.* **1996**, 3583−3598. (b) Cristiani, F.; Devillanova, F. A.; Isaia, F.; Lippollis, V.; Verani, G.; Demartin, F. *Polyhedron* **1995**, *14*, 2937−2943.
(7) (a) Demartin, F.; Deplano, P.; Devillanova, F. A.; Isaia, F.; Lippolis, V.; Verani, G. *Inorg. Chem.* **1993**, *32*, 3694−3699. (b) Cristiani, F.; Demartin, F.; Devillanova, F. A.; Isaia, F.; Saba, G.; Verani, G. *J. Chem. Soc., Dalton Trans.* **1992**, 3553−3560. (c) Freeman, F.; Ziller, J. W.; Po, H. N.; Keindl, M. C. *J. Am. Chem. Soc.* **1988**, *110*, 2586−2591. (d) Arzei, D.; Deplano, P.; Trogu, E. F.; Bigou, F.; Pellinghelli, M. A.; Vacca, A. *Can. J. Chem.* **1988**, *66*, 1483−1489.
(8) (a) Herbstein, F. H.; Schwotzer, W. *J. Am. Chem. Soc.* **1984**, *106*, 2367−2373. (b) Herbstein, F. H.; Schwotzer, W. *Angew. Chem., Int. Ed. Engl.* **1982**, *21*, 219−219. (c) Devillanova, F. A.; Verani, G. *Tetrahedron* **1979**, *35*, 511−514.
(9) (a) Foss, O.; Johnsen, J.; Tvedten, O. *Acta Chem. Scand.* **1958**, *12*, 1782−1798. (b) Hope, H.; Lin, H. Y. G. *Chem. Commun.* **1970**, 169−169. (c) Hope, H.; Lin, H. Y. G. *Acta Crystallogr., Sect. B* **1972**, *28*, 643−646.
(10) Aragoni, M. C.; Arca, M.; Demartin, F.; Devillanova, F. A.; Garau, A.; Isaia, F.; Lelj, F.; Lippolis, V.; Verani, G. *Chem.—Eur. J.* **2001**, *7*, 3122−3133 and reference therein.
(11) (a) Taurog A. *Endocrinology*; DeGroot, L., Ed.; Accademic Press: London, 1979; Vol. 1, p 331. (b) Morris, D. R.; Hager, L. P. *J. Biol. Chem.* **1966**, *241*, 3582−3589. (c) Nakataka, A.; Hidaka, H. *J. Clin. Endocrinol. Metab.* **1976**, *43*, 152−158.
(12) (a) du Mont, W. W.; Mugesh, G.; Wismach, C.; Jones, P. G. *Angew. Chem., Int. Ed.* **2001**, *40*, 2486−2489. (b) Berry, M. J.; Kieffer, J. D.; Harney, J. W.; Larsen, P. R. *J. Biol. Chem.* **1991**, *266*, 14155−14158. (c) Berry, M. J.; Banu, L.; Larsen, P. R. *Nature* **1991**, *349*, 438−440.
(13) Martidale. *The Extra Pharmacopoeia*, 28th ed.; Raynolds, J. E. F., Ed.; The Pharmaceutical Press: London, 1982.
(14) O'Brien, P. J. *Chem.-Biochem. Interact.* **2000**, *129*, 113−139.
(15) Rawitch, A. B.; Taurog, A.; Chernoff, S. B.; Dorris, M. L. *Arch. Biochem. Biophys.* **1979**, *194*, 244−257.
(16) (a) Magnusson, R. P.; Taurog, A.; Dorris, M. L. *J. Biol. Chem.* **1984**, *259*, 197−205. (b) Magnusson, R. P.; Taurog, A.; Dorris, M. L. *J. Biol. Chem.* **1984**, *259*, 13783−13790. (c) Huwiler, M.; Burgi, U.; Kohler, H. *Eur. J. Biochem.* **1985**, *147*, 469−476.

$$NMBZT + I_2 \rightarrow NMBZT{-}I_2 \qquad (1)$$

$$3NMBZT + 6I_2 + FeCl_3 \rightarrow$$
$$(1/2)[(NMBZT)_2I^+]{\cdot}[FeCl_4]^- + [(NMBZT)_2I^+]{\cdot}[I_7^-] +$$
$$(1/2)[FeCl_2]^+[I_3^-] \quad (2)$$

$$3MBZIM + 3I_2 \rightarrow \{[MBZIM{-}I_2]{\cdot}[(MBZIM)_2I]^+{\cdot}[I_3^-]\}$$
$$(3)$$

We recently showed that the reaction between MBZIM and I_2 in the ratio of 1:2 leads to the formation of the dimeric neutral complex $[\{(MBZIM)I_2\}_2{\cdot}I_2{\cdot}H_2O]^{1a}$ (eq 4). Demartin et al.[7a] isolated and characterized the ionic compound of formula $\{[(NMBZT)_2I]^+[I_7]^-\}$ (**2a**) derived from the reaction of NMBZT with I_2 in the molar ratio 1:2[7a] (eq 5). Cristiani et al.[6b] observed that when NMBZT and I_2 react in a molar ratio of 1:1, the neutral adduct $[(NMBZT){\cdot}I_2]$ (**1**) was obtained as a powder, together with crystals of $\{[(NMBZT)_2I]^+{-}[I_7]^-\}$.[6b]

$$MBZIM + 2I_2 \rightarrow [\{(MBZIM)I_2\}_2{\cdot}I_2{\cdot}H_2O] \qquad (4)$$

$$NMBZT + 2I_2 \rightarrow (1/2)[(NMBZT)_2I]^+{\cdot}[I_7^-] \ (\mathbf{2a}) \quad (5)$$

Thermal Analysis. Thermal analysis in flowing nitrogen showed that complexes **1** and **3** decompose in two stages. The TGA and DTA data curves for complex **1** show that the first stage of its decomposition sums up to a total of 89.8% mass loss and it is connected with two endothermic effects involving the stage between 94 and 182.00 °C that corresponds to 59.4% mass loss of iodine (the calculated mass loss is 58.4%), and this corresponds to an endothermic effect at 114.00 °C. The other stage is between 182 and 207.00 °C and corresponds also to an endothermic event at 206.68 °C and to 30.4% mass loss of the thione.

In complex **3**, two stages of decomposition occur in the range of 84.00−150.00 °C and correspond to 61.3% loss of iodine compared to the calculated 62.87% (endothermic 146.15 °C). The loss of thione involves 33% mass loss and occurs at 230.00−285.00 °C also accompanied with an endothermic event at 271.60 °C.

Conductivity Measurements. Conductometric titrations of NMBZT or MBZIM with I_2 in acetonitrile are shown in Figure 1.

At zero I_2 concentration, NMBZT solution (Figure 1A) has almost zero conductivity. This increases up to a higher value when the $[I_2]:[NMBZT]$ ratio is increased up to 2:1. This stoichiometry corresponds to complex $\{[(NMBZT)_2I]^+{\cdot}[I_7]^-\}$ (**2a**). Thus, when diiodine is added in the solution of NMBZT, initially both the neutral (**1**) and the ionic (**2a**) complexes may be formed as it is shown in Scheme 1A. Further addition of diiodine results to the formation of the ionic complex (**2a**) (Scheme 1A) when the $[I_2]:[NMBZT]$ molar ratio is 2:1. A similar interpretation is also valid for the reaction between MBZIM and I_2 resulting in the formation of the $\{[(MBZIM)_2I]^+{\cdot}I_3^-\}{\cdot}[(MBZIM)I_2]{\cdot}$**3** complex (Scheme 1B and Figure 1B).
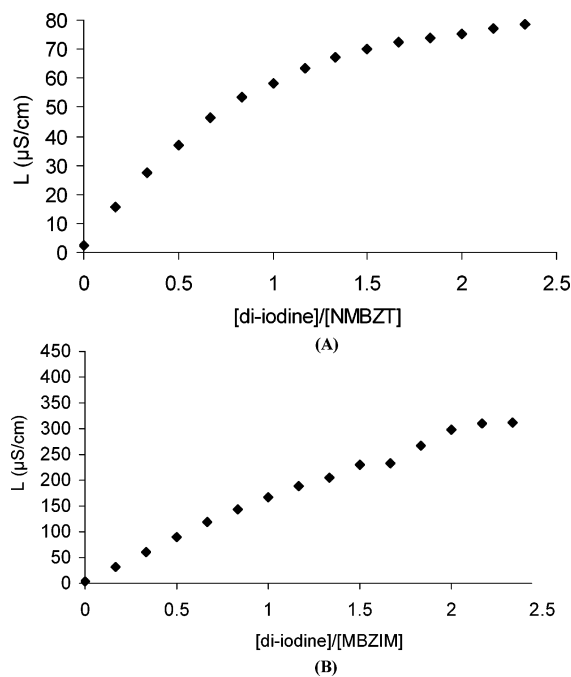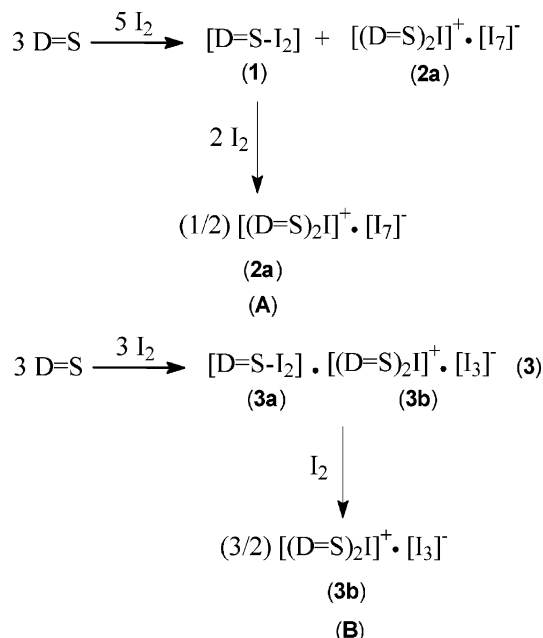

Figure 1. Conductivity titrations of NMBZT (A) or MBZIM (B), 10^{-2} M with I_2 in acetonitrile solutions ($T = 293$ K).

Scheme 1

Spectroscopy. (A) UV−Vis. The visible spectra of the thione−iodine adducts in dichloromethane or chloroform exhibit one distinct absorption band at 475−505 nm (476 for **1** and 496 nm for **3**), assigned to the "blue shift" band of I_2[8c] which appears at 504 nm in free I_2 in CH_2Cl_2.[7c] A shoulder in the range 310−360 nm of both compounds can be assigned to a charge-transfer band from the HOMO of the donor to the iodine LUMO $(\sigma_\pi{}^*)$.[3b,6a,8c] It should be noted that the ct (charge transfer) bands are not recognizable for complex **1** as they are most probably masked by the intraligand transitions ($\pi^* \leftarrow \pi$ or $\pi^* \leftarrow n$) occurring at almost the same wavelength. For complex **3** the ct band appears as a shoulder at 360 nm.

Table 1. Crystal Data and the Structure Refinement Details for the Complexes **1**−**3**

param	1	2	3
empirical formula	$C_8H_7I_2NS_2$	$C_{16}H_{14}IN_2S_4$, Cl_4Fe	$C_{21}H_{18}I_6N_6S_3$
fw	435.07	687.08	1212.03
cryst size, mm^3	$0.05 \times 0.2 \times 0.4$	$0.05 \times 0.31 \times 0.62$	$0.07 \times 0.1 \times 0.4$
cryst syst	orthorhombic	monoclinic	monoclinic
space group	$Pna2_1$	$C2/c$	$P2_1/n$
a, Å	12.5147(13)	35.781(2)	35.896(4)
b, Å	22.536(3)	7.4761(5)	4.7238(6)
c, Å	4.2994(5)	18.4677(12)	18.795(2)
β, deg	90	107.219(1)	97.325(11)
V, $Å^3$	1212.6(2)	4718.8(5)	3161.0(6)
Z	4	8	4
D_{calcd}, g cm^{-3}	2.383	1.934	2.547
μ, mm^{-1}	5.489	2.762	6.118
$R,^a$ $wR2^b$ [$I > 2\sigma(I)$], %	0.040, 0.030	0.060, 0.114	0.071, 0.109

^{a} $R = \Sigma||F_o| - |F_c||/\Sigma|F_o|$. ^{b} $wR2 = [\Sigma w(F_o^2 - F_c^2)^2/\Sigma w(F_o^2)^2]^{1/2}$.

(B) Vibrational Spectroscopy. The distinct vibrational bands in the ranges 1511−1457 and 1353−1313 cm^{-1} can be assigned to ν(CN) vibrations (thioamide I and II bands), and the bands 1048−1011 and 929−742 cm^{-1} can be attributed to the ν(CS) vibrations (thioamide III and IV bands). Amide N−CH_3 bond vibrations were observed at 1262 cm^{-1} for compound **1**, and ν(N−H) was observed at 3155 cm^{-1} in the case of **3**, which is shifted to higher wavenumber on passing from the free ligand to the complexes, typical behavior of sulfur donation. New bands appearing at 145 and 144 cm^{-1} in the far-IR spectra of compounds **1** and **3**, respectively, were assigned to the ν(I−I) stretching vibration modes.[1a,c]

The Raman spectra of complexes **1** and **3** were recorded in the 300−50 cm^{-1} region. The Raman spectrum of complex **1** shows an intense band at 160.50 cm^{-1} which can be attributed to the ν(I−I) vibration. Free iodine shows a band at 180 cm^{-1} for ν(I−I) in the solid state.[1a] This classifies compound **1** as the type D···I−I (A) with long D···I and short I−I bond distances according to the classification of Deplano et al.[5a] The spectrum of complex **3** shows a strong band at 108.43 cm^{-1} and a shoulder at 135.35 cm^{-1}. It is worth mentioning that bands around 110 cm^{-1} are normally attributed to the ν(I−I) stretching of symmetric I_3^-, which exhibits only one Raman active band.[1a−1c,3a] For asymmetric I_3^-, bands assigned to ν(I−I) are observed at higher (140−130 cm^{-1}) frequencies (135.5 cm^{-1} in the present case). At lower frequencies (80−70 cm^{-1}) deformation motions are also observed (in our case this band has not been observed most probably because it is masked by the very intense band at 108.43 cm^{-1}). Thus, the complex should contain a symmetric and an asymmetric I_3^- unit[3a] as confirmed by the crystallographic study.

Crystal and Molecular Structures. Dark crystals of the complexes suitable for X-ray single-crystal analysis were grown by slow evaporation of the filtrates yielded from the reaction of diiodine with the appropriate ligand in dichloromethane solution. Representations of complexes **1**−**3** are shown in Figures 2−4. Crystal data and the structure refinement details are given in Table 1, and selected bond lengths and angles are given in Tables 2−4.

(i) Structure of [(NMBZT)·I_2] (1). The crystal structure of compound **1** comprises a thione ligand, bonded with a

Table 2. Selected Bond Lengths (Å) and Angles (deg) for Compound **1**

	Bond Lengths		
I(1)−I(2)	2.7914(9)	I(1)−S(2)	2.808(3)
S(1)−C(2)	1.714(8)	S(1)−C(7A)	1.739(9)
S(2)−C(2)	1.698(9)	N(3)−C(2)	1.344(9)
N(3)−C(3)	1.460(7)	N(3)−C(3A)	1.402(10)
C(3A)−C(4)	1.378(11)	C(3A)−C(7A)	1.395(10)
C(4)−C(5)	1.395(12)	C(5)−C(6)	1.393(11)
C(6)−C(7)	1.359(12)	C(7)−C(7A)	1.380(10)

	Angles		
I(2)−I(1)−S(2)	176.94(6)	C(2)−S(1)−C(7A)	92.3(5)
S(1)−C(2)−N(3)	112.5(7)	S(2)−C(2)−N(3)	123.4(7)
S(1)−C(2)−S(2)	124.1(6)	I(1)−S(2)−C(2)	104.4(3)
C(2)−N(3)−C(3)	122.5(8)	C(3)−N(3)−C(3A)	125.1(8)

	Torsion Angles		
N(3)−C(2)−S(2)−I(1)	172.7(7)	S(1)−C(2)−S(2)−I(1)	−9.0(6)
I(2)−I(1)−S(2)−C(2)	163.1(12)	S(2)−C(2)−N(3)−C(3A)	178.6(6)

Table 3. Selected Bond Lengths (Å) and Angles (deg) for Compound **2**

	Bond Lengths		
I(1)−S(1)	2.5961(15)	I(1)−S(3)	2.6596(14)
S(1)−C(1)	1.704(6)	S(2)−C(1)	1.719(6)
S(2)−C(8)	1.737(6)	S(3)−C(9)	1.703(5)
S(4)−C(9)	1.713(5)	N(1)−C(1)	1.333(7)
N(1)−C(2)	1.475(7)	N(1)−C(3)	1.398(7)
Fe−Cl(1)	2.2049(17)	Fe−Cl(2)	2.1887(17)
Fe−Cl(3)	2.1877(18)	Fe−Cl(4)	2.1973(17)

	Angles		
S(1)−I(1)−S(3)	177.77(5)	I(1)−S(1)−C(1)	100.4(2)
I(1)−S(3)−C(9)	104.14(19)	Cl(1)−Fe−Cl(2)	111.86(7)
Cl(1)−Fe−Cl(3)	108.43(8)	Cl(1)−Fe−Cl(4)	105.73(7)
Cl(2)−Fe−Cl(3)	107.44(7)	Cl(2)−Fe−Cl(4)	113.03(7)
Cl(3)−Fe−Cl(4)	110.30(7)		

	Torsion Angles		
I(1)−S(3)−C(9)−S(4)	−3.0(4)	I(1)−S(1)−C(1)−S(2)	−15.8(4)

diiodine atom through sulfur with I(1)−S(2) = 2.808(3) Å (Figure 2A). The S−I bond distance found in **1** is among the longest ever measured for such type of adduct indicating a relatively weak interaction between thioamide and diiodine (Table 5). From the data collected in Table 5, the range of S−I bond lengths is 2.571(6) Å, in [{(bzimtH)I_2}$_2$·I_2·2H_2O][1a] to 2.874(2) Å, in [bzoxtH·I_2].[6b]

The corresponding I−I bond distance of 2.7914(9) Å is longer than the I−I distances either in the gas phase (2.677 Å)[7c,17a,18] or in crystalline diiodine (2.717(6) Å at 110 K)[7c,17b] as a result of the presence of the S···I interaction. On the

Table 4. Selected Bond Lengths (Å) and Angles (deg) for Compound **3**

<div align="center">Bond Lengths</div>

I(1)−I(2)	2.9300(12)	I(1AA)−I(2AA)	2.880(6)
I(1AA)−I(3AA)	3.058(5)	I(321)−I(322)	2.8869(13)
I(11)−S(12)	2.597(4)	I(11)−S(22)	2.702(4)
I(321)−S(32)	2.670(4)	S(12)−C(12)	1.666(15)
S(22)−C(22)	1.692(13)	S(32)−C(32)	1.681(14)
N(11)−C(12)	1.362(15)	N(13)−C(12)	1.336(17)
N(21)−C(22)	1.336(15)	N(23)−C(22)	1.332(15)
N(31)−C(32)	1.340(14)	N(33)−C(32)	1.357(16)

<div align="center">Angles</div>

I(2AA)−I(1AA)−I(3AA)	178.45(12)	S(12)−I(11)−S(22)	171.32(12)
I(322)−I(321)−S(32)	178.35(10)	I(11)−S(12)−C(12)	105.2(5)
I(11)−S(22)−C(22)	108.2(5)	I(321)−S(32)−C(32)	102.7(5)
S(12)−C(12)−N(11)	126.0(11)	S(22)−C(22)−N(21)	122.9(11)
S(32)−C(32)−N(31)	131.1(10)		

<div align="center">Torsion Angles</div>

I(11)−S(12)−C(12)−N(13)	69.6(13)	S(22)−I(11)−S(12)−C(12)	146.4(8)
S(12)−I(11)−S(22)−C(22)	164.1(8)	N(31)−C(32)−S(32)−I(321)	−2.5(14)
N(23)−C(22)−S(22)−I(11)	−2.1(13)		

basis of the values of the I−I bond order (n) defined by Pauling,[17a] $d(\text{I}-\text{I}) = d_o - 0.85 \log(n)$ (where d_o is the I−I bond distance of the I_2 in the gas phase, which is 2.67 Å [18]), Bigoli et al.[6a] classified I_2 adducts into three groups, i.e., A−C types. When the value of the I−I bond order (n) ≥ 0.6, corresponding to $d(\text{I}-\text{I})$ < 2.85 Å, the adduct is classified as an A type, and when n ≤ 0.4 ($d(\text{I}-\text{I})$ > 3.01 Å), the C type is determined.[6a] Compounds with intermediate values are of B type.[6a] Thus, compound **1** is classified as an A type, consistent with a weak S···I−I interaction.

The linearity of the S(2)−I(1)−I(2) atoms, angle = 176.94(6)°, coupled with the value of the N(3)−C(2)−S(2)−I(1) torsion angle of 172.7(7)° highlights the planarity of **1**.

In the crystal structure of **1**, a layer structure is formed as a result of extensive hydrogen-bonding interactions, as illustrated in Figure 2A. The layer may be thought of being comprised of interconnected cyclotetrameric units of **1** sharing a 32-membered [IISCSCCH]₄ ring held together by I···H contacts: C(3)−H···I(2)ⁱ = 3.01 Å and C(3)···I(2)ⁱ = 3.701(9) Å with the angle at H being 130° and C(7)−H··· I(1)ⁱⁱ = 3.53 Å and C(7)−H···I(1) 3.962(11) Å with angle 133° for symmetry operations i, $-1/2 + x$, $-1\frac{1}{2} + y$, $-1 + z$, and ii, $1/2 + x$, $-1\frac{1}{2} + y$, $-1 + z$. An alternate description of the layer arrangement is one in which successive rows of molecules mediated by I···H$_\text{methyl}$ interactions are linked via H···H$_\text{phenyl}$ interactions.

(ii) Structure of {[(NMBZT)₂I⁺]·[FeCl₄]⁻ (2). The structure of compound **2** comprises cationic {(NMBZT)₂I⁺}, containing a linear S−I⁺−S linkage, and [FeCl₄]⁻ as a counteranion, as shown in Figure 3A. There are only a few reports dealing with crystal structures of iodonium salts. Examples include [{(tzdtH)₂I⁺}·I₃⁻·2I₂],[1a] {[(dmtu)₂I]},[4b] [(tu)₂I⁺],[9b,c] [(etu)·I⁺],[8a,b] and {[(NMBZT)₂I⁺]·[I₇]⁻.[7a]

The S−I bond lengths found in **2** are unequal: I(1)−S(1) = 2.5961(15) and I(1)−S(3) = 2.6596(14) Å. Disparate bond distances are found also in {[(NMBZT)₂I⁺]·[I₇] (I−S =

2.600(2) and 2.634(2) Å)[7a] and {[(dmtu)₂I]} (S−I = 2.602(4) and 2.654(4) Å[4b]). By contrast, equal S−I bond distances are found in [{(tzdtH)₂I⁺}·I₃⁻·2I₂][1a] of 2.654(6) Å and [(tu)₂I⁺] of 2.629 Å[9b,c] which are significantly longer than those in (etu)·I⁺, i.e., 2.487(3) Å.[8a,8b] The S−C bond lengths of complex **2** are 1.704(6) and 1.703(5) Å, while those found in {[(NMBZT)₂I⁺]·[I₇] } are C=S = 1.694(7) and 1.682(7) Å.[7a] The S(1)−I(1)−S(3) bond angle is 177.77(5)°, indicating linearity, but the overall molecule is not planar as seen by the value of the I(1)−S(1)−C(1)−S(2) torsion angle I of −15.8(4)°.

The constituent ions of **2** associate via Fe−Cl···H interactions with the closest such interaction being 2.88 Å between Cl(3) and H(4)ⁱ for i, $1/2 - x$, $1/2 - y$, $1 - z$. As emphasized in Figure 3B, there are stacking interactions between the five- and six-membered rings of the thione containing the S(1) atom so that the separation between the centrosymmetrically related rings is 3.742(3) Å, indicating a head to head arrangement of the two ligands.

The Fe−Cl bond distance of the effectively tetrahedral [FeCl₄]⁻ counteranion varies from 2.1887(17) to 2.2049(17) Å while the bond angles range from 105.73(7) to 113.03(7)°.

(iii) Structure of {[(MBZIM)₂I⁺]·I₃⁻]·[(MBZIM)I₂]·3. The spoke−ionic mixed complex {[(MBZIM)₂I]⁺·[I₃]⁻}· [(MBZIM)I₂]·**3** is formed when benzimidazole-2-thione reacts with diiodine in a molar ratio of 1:1. The structure comprises two components, one molecular diiodine adduct [(MBZIM)I₂] (**3a**) and one ionic adduct {[(MBZIM)₂I]⁺·[I₃]⁻} (**3b**). Although ionic and spoke structures have been reported to exist simultaneously in solution,[4b,6b,7c] this is observed, to our knowledge for the first time, in the solid state in **3**.

The structure of the neutral constituent of **3**, [(MBZIM)- I₂] (**3a**), comprises a thione ligand bonded to one of the iodine atoms through sulfur so that the I(321)−S(32) distance of 2.670(4) Å falls within the expected range (Table 5). The I(321)−I(322) bond distance is 2.8869(13) Å, which is elongated owing to the formation of the I−S bond and, therefore, is classified as the B type according to the Bigoli et al.[6a] classification (Table 5). As for **1**, the molecule is

(17) (a) Pauling, L. *The Nature of the Chemical Bond*, 3rd ed.; Cornell University Press: Ithaca, NY, 1960. (b) Van Bolhuis, F.; Koster, P. B.; Migchelsen, T. *Acta Crystallogr.* **1967**, *23*, 90.
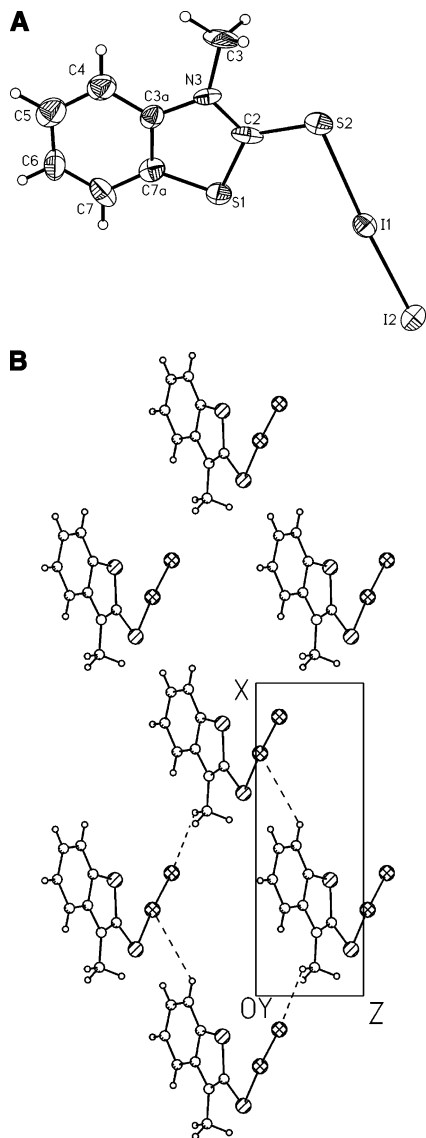(18) Burgi, H. B. *Angew. Chem., Int. Ed.* **1975**, *14*, 460−473.

Figure 2. ORTEP diagram (A) and unit cell (B) of the neutral compound **1** showing the atomic numbering scheme.

essentially planar as seen in the magnitude of the N(31)−C(32)−S(32)−I(321) torsion angle of −2.5(14)°.

The structure of the ionic component, **3b**, of **3** comprises two residues, one cationic {(MBZIM)$_2$I$^+$}, containing the linear S(22)−I$^+$−S(12) linkage, Figure 4A, and a I$_3$$^-$ counteranion. The I$_3$$^-$ counteranion exists as two independent entities, one ordered and the other not. The ordered component, containing I1 and I2, is disposed about a center of inversion and has equal I−I bonds I(1)−I(2) = 2.9300(12) Å. The second component of the anion comprises three atoms, i.e., I1AA−I3AA, each of half weight, and after the application of (centro)symmetry, results in the formation of a chain of iodide atoms along the *b*-axis (see Experimental Section). The I(1AA)−I(2AA) bond distance is 2.880(6) Å, and that of I(1AA)−I(3AA) is 3.058(5) Å, indicating asymmetry. These interactions are classified as the B type for the first I$_3$$^-$ ion and C type for the second[6a] (Table 5). The S−I bond lengths are I(11)−S(12) = 2.597(4) and I(11)−S(22) = 2.702(4) Å, and the S(12)−I(11)−S(22) bond
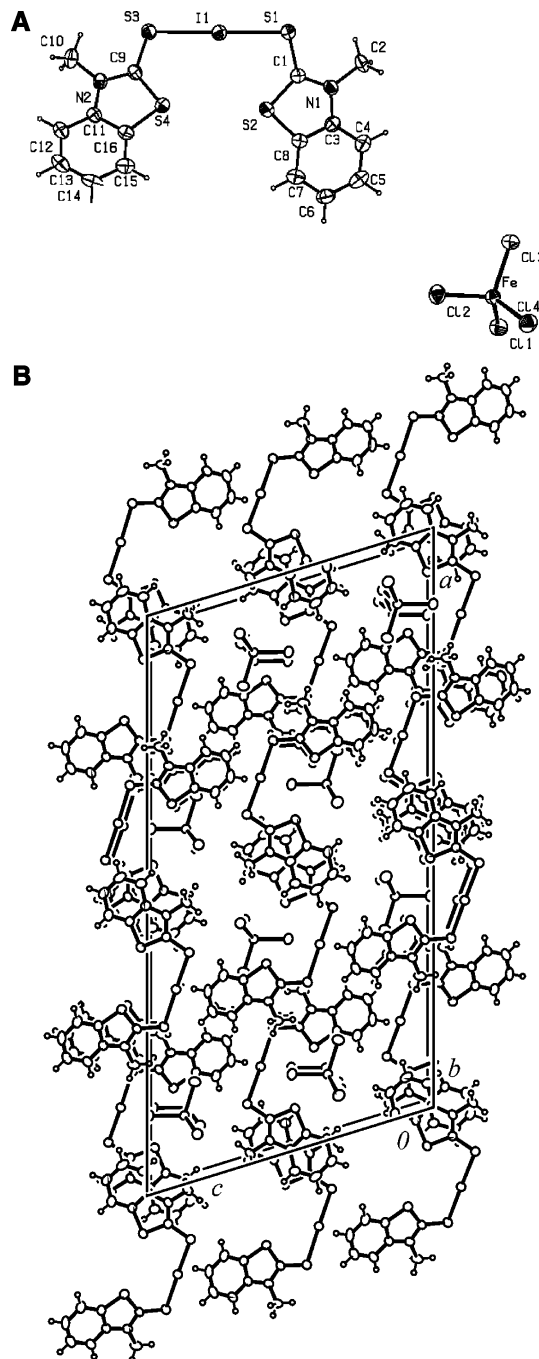
Figure 3. ORTEP diagram (A) and unit cell (B) of the ionic components of compound **2** showing with the atomic numbering scheme.

angle is 171.32(12)°, i.e., somewhat deviated from linearity. This deviation may be ascribed to intermolecular interactions between the central I(11) atom and N(11)H atoms of the cations; see Figure 4B. In the cation, the S−I bond lengths are I(11)−S(12) = 2.597(4) and I(11)−S(22) = 2.702(4) Å, and the S(12)−I(11)-S(22) bond angle is 171.32(12)°, i.e., somewhat deviated from linearity. This deviation may be ascribed to intermolecular interactions between the central I(11) atom and N(11)H atoms, derived from a symmetry-related cation. The shortest such contact is I(11)···H−N(11)^{ii} of 3.20 Å, I(11)···N(11)^{ii} is 3.975(11) Å, and the angle at H is 152° (symmetry transformation ii: $^1/_2$ − x, $^1/_2$ + y, $1^1/_2$ − z). Additionally, weaker I(11)···H−N(11) interactions

Table 5. Structural Data of Some Iodine Complexes with Heterocyclic Thioamides

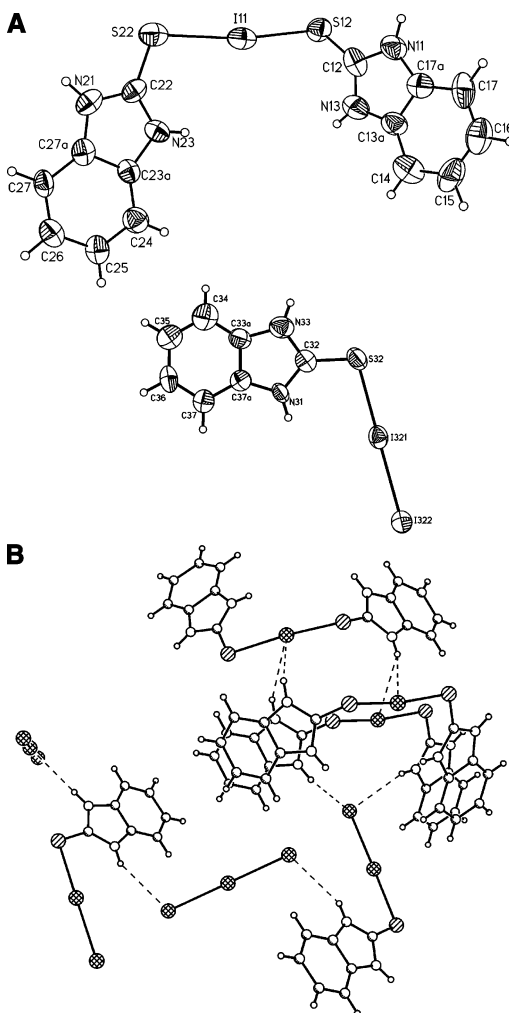| compound	structure	$d(I-S)$ (Å)	$d(I-I)$ (Å)	$d(C=S)$ (Å)	$I-I$ bond order (n)	type (A) ($n \geq 0.6$ or $d(I-I) < 2.85$ Å) (B) ($0.6 \geq n \geq 0.4$ or $3.01 > d(I-I) > 2.85$ Å) (C) ($n \leq 0.4$ or $d(I-I) > 3.01$ Å)	ref
$[(NMBZT) \cdot I_2]$ (**1**)	spoke	2.808(3)	2.7912(9)	1.716(8)	0.720	A	b
$\{[(NMBZT)_2I^+\} \cdot [FeCl_4]^-$ (**2**)	iodonium salt	2.5961(15), 2.6596(14)	↔	1.704(6), 1.703(5)	↔		b
$\{[(MBZIM)_2I^+\} \cdot I_3^-\} \cdot [(MBZIM)I_2]$ (**3**)	mixed iodonium salt **3b** and spoke **3a**						
$\{[(MBZIM)_2I^+\} \cdot I_3^-\}$ (**3b**)		**3b:** 2.597(4), 2.702(4)	**3b**(I_3^- or $I^-\cdots I_2$): 2.9300(12), 2.9300(12), 2.880(6), 3.058(5)	**3b:** 1.666(15), 1.692(13)	**3b**(I_3^- or $I^-\cdots I_2$): 0.494, 0.566, 0.350	**3b**(I_3^- or $I^-\cdots I_2$): B, B,C	b
$[(MBZIM)I_2]$ (**3a**)		**3a:** 2.670(4), 2.654(6)	**3a**(I_2): 2.8869(13); (I_3^- or $I^-\cdots I_2$): 2.9195(14)	**3a:** 1.681(14), 1.65(3)	**3a**(I_2): 0.556; (I_3^-): 0.509	**3a**(I_2): B; (I_3^- or $I^-\cdots I_2$): B	b
$[\{(tzdtH)_2I^+\} \cdot I_3^- \cdot 2I_2]^a$	iodonium salt	2.587(5)	2.969(2)	1.706(18)	0.445	B	1a
$[\{(bztzdtH)_2\} \cdot I_2]^a$	extended spoke	2.728(6)	3.077(2)	1.75(2)	0.332	C	1a
$[(bztzdtH)I_2]^a$	spoke	2.571(6)	2.989(2)	1.722(19)	0.421	B	1a
$[\{(bzimtH)I_2\}_2 \cdot I_2 \cdot 2H_2O]^a$	spoke	2.7805(10)	2.8264(4)	1.696(4)	0.655	A	1c
$[(PTU)I_2]^a$	spoke	2.634(2)	2.9205(7)	1.680(6)	0.507	B	1c
$[CMBZT)I_2]^a$	spoke						
$\{(PYS-PYSH)^+ \cdot I_3^-\}^a$ four molecules in unit cells a−d	cationic disulfide	↔	(I_3^- or $I^-\cdots I_2$): (a) 2.887(4), 2.944(3); (b) 2.874(4), 2.957(3); (c) 2.968(3), 2.862(4); (d) 2.855(4), 2.927(3)	(a) 1.85(3), 1.77(3); (b) 1.78(3), 1.75(3); (c) 1.65(2), 1.77(3); (d) 1.71(2), 1.69(3)	(I_3^- or $I^-\cdots I_2$): 0.556, 0.476; 0.575, 0.460; 0.446, 0.594; 0.606, 0.498	(I_3^- or $I^-\cdots I_2$): B, B; B, B; B, B; A,B	1d

Figure 4. ORTEP diagram (A) and unit cell (B) of the ionic and neutral components of compound **3** showing with the atomic numbering scheme.

Figure 5. Correlation of $d(I-I)$ vs $d(I-S)$ bond distances found in complexes **1**, **3b**, [{(bztzdtH)I$_2$}·I$_2$] (**4**),[1a] [(bztzdtH)I$_2$] (**5**),[1a] [{(bzimtH)-I$_2$}$_2$·I$_2$·2H$_2$O] (**6**),[1a] [(PTU)I$_2$] (**7**),[1c] and [(CMBZT)I$_2$] (**8**)[1c] with "spoke" or "extended spoke" structures.

Figure 5 correlates the $d(I-I)$ vs $d(I-S)$ bond distances found in complexes **1**, **3b**, [{(bztzdtH)I$_2$}·I$_2$] (**4**),[1a] [(bztzdtH)-I$_2$] (**5**),[1a] [{(bzimtH)I$_2$}$_2$·I$_2$·2H$_2$O] (**6**),[1a] [(PTU)I$_2$] (**7**),[1c] and [(CMBZT)I$_2$] (**8**)[1c] with "spoke" or "extended spoke" structures. According to the graph, the antithyroid drug PTU as well as the thioamide NMBZT interact with diiodine to form weak ct complexes. Therefore, they function in the same way so as to may interfere with the mechanism of thyroid hormones synthesis (see Conclusions).

Computational Studies. To investigate further the nature of bonding in the diiodine adducts, computational studies using ab initio quantum mechanical methods and density functional theory (DFT) techniques have been performed for the [(MBZT)I$_2$],[1a] [(NMBZT)I$_2$] (**1**), [(MBZIM)I$_2$] (**3a**), and {[MBZIM)$_2$I$^+$]I$_3^-$} (**3b**) species. A first theoretical study on these systems was carried out by Laurence et al.,[19a] who performed a semiempirical PM3 modeling of the methimazole—I$_2$ complex and showed quantitatively the interesting ct character of these species. Very recently Aragoni et al.[19b] have made an extensive investigation of the related [LEX]$^+$ systems (LE = N,N-dimethylbenzoimidazole-2(3H)-thione and -2(3H)-selone, X = I, Br). Their NBO charge distribution analysis supported that the most likely products from the reactions of these ligands with IBr are the LEX$_2$ ct adducts and the T-shape hypervalent adducts which feature a linear Br—Se—I geometry. The present investigation of the first three adducts of the type D···I$_2$ demonstrates quantitatively several common geometrical features and, in particular, the effect of the hydrogen bonding upon the geometry when the amidic hydrogen is substituted by the methyl group. The calculations on [(MBZIM)I$_2$] (**3a**) and {[MBZIM)$_2$]$^+$[I$_3$]$^-$} (**3b**) allow the comparison of the energetics and give evidence for the relative stability of **3b**.

Selected bond distances obtained from the theoretical study are summarized in Table 6. In general, the calculated results are consistent with the geometrical features observed experimentally. Thus, planar molecular geometries are obtained for [(MBZT)I$_2$], [(NMBZT)I$_2$] (**1**), and [(MBZIM)I$_2$] (**3a**) with no appreciable change in the C=S bond distances and

are found (I(11)···H—N(11)^{iii} = 3.55 Å, I(11)···N(11)^{iii} = 3.940(11) Å, and the angle at H is 111° (symmetry transformation iii: $^1/_2 - x$, $-^1/_2 + y$, $1^1/_2 - z$) that work in a cooperative fashion to link cations into a double chain, directed along the b-axis, as shown in Figure 4B. Finally, the cation is not planar as evidenced from the I(11)—S(12)—C(12)—N(13) torsion angle of 69.6(13)°.

In addition to the I···H hydrogen bonds mentioned above, there are other hydrogen-bonding interactions operating in the lattice of **3**. A second discernible chain is evident in that lattice that comprises the two independent I$_3^-$ counteranions and the [(MBZIM)I$_2$] molecules mediated by N31—H···I(1)^{iv} interactions (2.92 Å, 3.696(9) Å, and 151° for iv: $^1/_2 - x$, $^1/_2 + y$, $^1/_2 - z$) and N33—H···I(1AA) interactions (2.73 Å, 3.578(11) Å, and 172°). The chains, oriented along the c-direction, are orthogonal to the aforementioned double chain, and the links between them involve the terminal I(322) atom that forms two interactions to two N—H atoms derived from one cation, i.e., N(13)—H^v (2.95 Å, 3.581(11) Å, 132° for v: $1 - x$, $1 - y$, $2 - z$) and N(23)—H^v (2.88 Å, 3.626(11) Å, 146°). In this way, the I(322) atom closes a 10-membered, hydrogen-bond mediated [I···HNCSISCNI···] ring. The different hydrogen-bonding interactions operating in the structure of **3** are illustrated in Figure 4B.
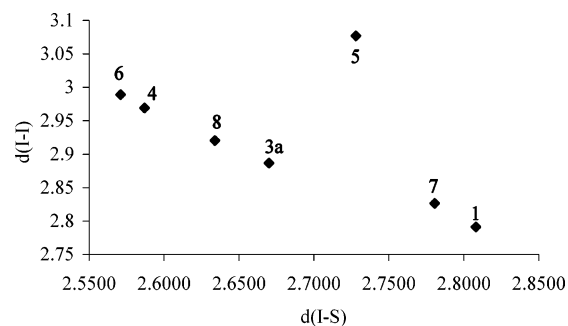
(19) (a) Laurence, C.; El Ghomari, M. J.; Le Questel, J.-Y.; Berthelot, M.; Mokhlisse, R. *J. Chem. Soc., Perkin Trans.* **1998**, *2*, 1545−1551. (b) Aragoni, M. C.; Arca, M.; Demartin, F.; Devillanova, F. A.; Garau, A.; Isaia, F.; Lippolis, V.; Verani, G. *J. Chem. Soc, Dalton Trans.* **2005**, 2252−2258

Table 6. Selected Theoretical Bond Lengths r (Å) and Electronic Energies E (hartree)

R	[(MBZT)I$_2$]	[(NMBZT)I$_2$] (1)	[(MBZIM)I$_2$] (3b)	{[(MBZIM)$_2$I$^+$]I$_3^-$} (3a)
I−I	2.976	2.962	2.986	3.268,^{a} 3.011^a
S−I	3.069	3.065	3.039	2.832
C−S	1.723	1.726	1.744	1.770
E			−412.722 38	−825.455 035

^{a} These bond distances correspond to the (I···I−I)$^-$ counteranion.

Table 7. Mulliken Atomic Charges on Selected Atoms for the Four Compounds Investigated

[(NMBZT)I$_2$] (1)		[(MBZIM)I$_2$] (3a)		{[(MBZIM)$_2$I$^+$]I$_3^-$} (3b)	
atom^a	atomic charges	atom^b	atomic charges	atom^b	atomic charges
I(1)	−0.029	I(321)	−0.051	I(11)	+0.066
I(2)	−0.184	I(322)	−0.205	I(2ÀA)^c	−0.468,
S(2)	−0.020	S(32)	−0.027	I(1AA)^c	−0.107
S(1)	+0.358	C(32)	−0.155	I(3AA)^c	−0.250
C(2)	−0.383	N(31), N(33)	−0.329, −0.349	S(12), S(22)	−0.043, −0.021
N(3)	−0.105	H,^{d} H^d	+0.348, +0.364	C(12), C(22)	−0.092, −0.153
		C(32a)	+0.252	C(17a), C(27a)	+0.247, +0.242
		C(37a)	+0.257	C(13a), C(23a)	+0.248, +0.243
				N(11), N(21)	−0.356, −0.256
				H,^{d} H^d	+0.351, +0.242
				N(13), N(23)	−0.337, −0.292
				H,^{d} H^d	+0.333, +0.280

^{a} Atomic labeling given is in agreement with the corresponding labeling showing in Figure 2A. ^{b} Atomic labeling given is in agreement with the corresponding labeling showing in Figure 4A. ^{c} These atomic charges correspond to the (I···I−I)$^-$ counteranion. ^{d} Amidic hydrogen.

a considerable lengthening of the diiodine bond by more than 10% upon complexation compared to the bond distance in gas-phase, i.e., unassociated, I$_2$ of 2.677 Å.[17a,18] A near linear S···I−I arrangement is found with S···I distances ranging from 3.069 to 3.039 Å, i.e., within the region 3.10−2.58 Å, which characterizes this series of compounds.[19a] Thus, the calculated S−I and I−I bond distances are consistent with the B type classification[6a] for compounds [(MBZT)I$_2$][1a] and [(MBZIM)I$_2$] (**3a**). Intramolecular hydrogen bonding is found in the solid-state [(MBZT)I$_2$][1a] and [(MBZIM)I$_2$] (**3a**) complexes, each formed between the amidic hydrogen and the sulfur bonded iodine atom with H···I distances 2.82 and 2.89 Å, respectively. The hydrogen bonding (i) confirms the negative charge character of the I atom[19a] within the same molecule and (ii) greatly influences the geometry adopted by the molecule. Thus, the C=S···I angle takes the values 98.8 and 99.4° for [(MBZT)I$_2$] and [(MBZIM)I$_2$] (**3a**), respectively, with the S···I−I axis oriented toward the amidic hydrogen. In [(NMBZT)I$_2$] (**1**), the C=S···I angle is found to be 105.4° with the S···I−I axis oriented away from the side crowded with the methyl group.

The fourth complex studied theoretically, {[(MBZIM)$_2$I]$^+$-[I$_3$]$^-$} (**3b**), belongs to the iodonium salt type of diiodine adducts. It shows a C=S···I angle similar to that for **1**, i.e., 101.5°, and a significant shortening of the S−I distance, reflecting the greater stability of the S−I bond in **3b** compared to the stability of the analogous bond in D···I$_2$ complexes. The effect is supported quantitatively by considering the energy difference calculated at the Hartree−Fock level of theory for the constituents of the corresponding disproportionation reaction (Schemes 1 and 2). Thus, {[(MBZIM)$_2$I$^+$]I$_3^-$} (**3b**) is more stable than 2 × [(MBZIM)-I$_2$] (**3a**) by about 6 kcal mol^{-1}. Although the theoretical energy difference represents only gas-phase results and there are additional entropic factors that influence the dispropor-
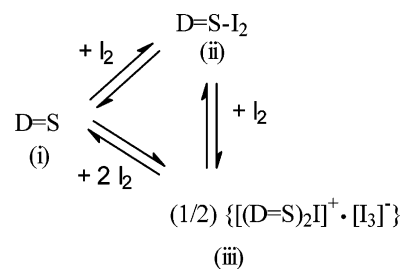
Scheme 2

tionation transformation reaction (Scheme 2), the calculated greater stability of the ionic adduct is, nevertheless, a major driving force which contributes significantly to the stabilization of the ionic-type compounds {[D$_2$I$^+$][I$_3^-$]}.

Consideration of the Mulliken atomic charges listed in Table 7 provides evidence for the nature of the intermolecular interactions that produce the specific conformations obtained in the solid state, shown in Figures 2B and 4B. The Spoke structures [(MBZT)I$_2$], [(NMBZT)I$_2$] (**1**), and [(MBZIM)I$_2$] (**3a**) are obviously held together in the crystalline state by hydrogen-bonding interactions between the electron-deficient amidic, methyl, or aromatic hydrogen atoms and the electronegative iodine atoms as it is nicely shown in Figure 2B. However, in the case of the iodonium salt, {[(MBZIM)$_2$I]$^+$-[I$_3$]$^-$} (**3b**), the situation is different because the bridged iodine atoms in the S−I−S unit are found to be positively charged. Therefore, in the case of the iodonium salts it is suggested that the conformations obtained in the crystalline state result from a intermolecular electrostatic interaction between the positively charged iodine and the negatively charged NH group (total group (NH) charges calculated −0.005, −0.014, −0.004, and −0.012 e).

In summary, the theoretical results of the gas-phase sulfur−iodine charge-transfer complexes are consistent with the experimental findings, confirming the moderate S···I and

I···I intramolecular coupling and suggesting the type of intermolecular interactions, on the basis of the atomic charges, between different molecular units which produce the conformations obtained in the solid state. More specifically, hydrogen bonding is suggested to be responsible for the solid-state conformations in the case of "spoke" type complexes, while electrostatic type attractions are suggested to produce the solid-state conformations in the case of the iodonium salts. Finally, the theoretical calculations predict the considerable stabilization for the ionic $\{[(MBZIM)_2I^+]I_3^-\}$ (**3b**) compound in the disproportionation showing in Scheme 2 on the basis of the calculated electronic energy values.

Conclusions

Boyle et al.,[4b] on the basis of Raman spectroscopy and X-ray crystal structure determinations, concluded that the formation of "spoke" structures of thiones with I_2 depends solely on the donor strength of thione. Thus, weak donors such as thiourea (tu) form ionic compounds, while stronger donors such as *N*-methyl-2-mercaptobenzothiazole (NMBZT) form "spoke" structures alone. However, Deplano et al.[7a] isolated and characterized the iodonium salt $\{[NMBZT)_2I]^+$-$[I_7^-]\}$. In the present study, complex **3**, of formula $\{[(MBZIM)_2I]^+\}\cdot[I_3^-]\cdot[(MBZIM)I_2]$, isolated from the reaction 2-mercaptobenzimidazole and I_2, reveals the cocrystallization of both a "spoke" structure and an iodonium structure. This leads to the conclusion that the equilibrium shown in Scheme 2 is established in solution. Thus, on passing initially from the "spoke" structure, the iodonium salt in excess of I_2 results. This is also supported by the conductivity measurements. It has also been shown that the disproportionation reaction, with the generation of the ionic compound from thioamide−iodine complexes, exhibits pressure dependence.[1b] A pressure increase leads to the ionic iodonium salt (iii) from (ii) (Scheme 2). The favoring of $\{[(MBZIM)_2I]^+[I_3^-]\}$ formation is also proved by computational studies, on the basis of energetic grounds.

Computational studies also confirm (a) the lengthening of the I−I bond distance as compared to the I−I bond length in free iodine molecule, (b) the intramolecular hydrogen-bonding effect in $[(MBZT)I_2]$ and $[(MBZIM)I_2]$ geometries, and (c) the possible intermolecular interactions that may be responsible for the type of conformations obtained in the solid state.

Scheme 3 summarizes a possible inhibition mechanism of TPO-catalyzed iodination reactions.[1c,4a,12] Thus, thioamides exhibiting antithyroidal activity against hyperthyroidism (Graves' disease) can be classified now into two categories: (i) thioamides which react with diiodine, forming mono- and dicationic salts, like MMI[4a] and (ii) thioamides able to form weak charge-transfer compounds with diiodine, like PTU.[1c] Thus, it seems that drugs such as MMI, etc., proposed to interfere with the iodination mechanism in their ability to form the active iodine species, compete with tyrosil residues of thyroglobuline for the active iodine[4a,12] (Scheme 3). 2-Mercaptopyridine (PYSH) may also be a molecule that functions similarly.[1d] Drugs such as PTU, on the other hand, function instead by their ability to inhibit the activity of

Scheme 3. Possible Inhibition Mechanism of TPO-Catalyzed Iodination Reactions (MIT = 3-Monoiodotyrosine and DIT = 3,5-Diiodotyrosine)
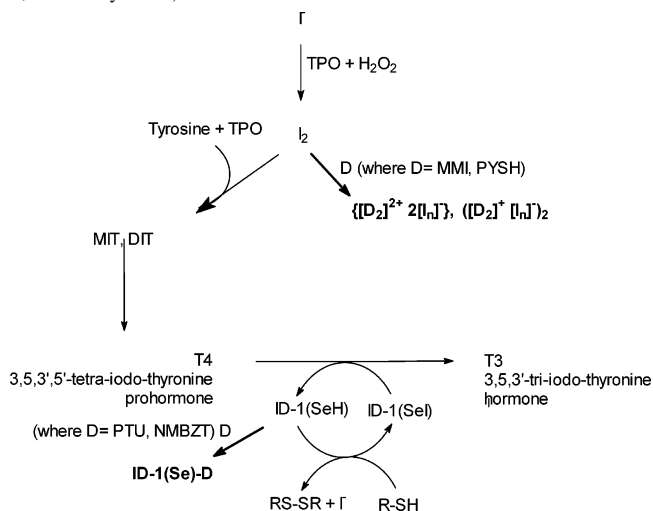
iodothyronine deiodinase (ID-1), an enzyme responsible for the monodeiodination of the T4 prohormone to the T3 hormone (Scheme 3). In this category of drug, NMBZT may also be active.

Experimental Section

Materials and Instruments. All solvents used were of reagent grade. Diiodine (Aldrich), *N*-methylbenzothiazole-2-thione, and benzimidazole-2-thione (Aldrich, Merk) were used with no further purification. Elemental analyses for C, H, N, and S were carried out with a Carlo Erba EA model 1108 elemental analyzer. Melting points were measured in open tubes with a Stuart scientific apparatus and are uncorrected. Infrared spectra in the region of $4000-370$ cm^{-1} were obtained in KBr disks while far-infrared spectra in the region of $400-50$ cm^{-1} were obtained in polyethylene disks, with a Perkin-Elmer Spectrum GX FT-IR spectrophotometer. A Jasco UV/vis/NIR V 570 series spectrophotometer was used to obtain the electronic absorption spectra. The ^{1}H NMR spectra were recorded on a Bruker AC250 MHFT-NMR instrument in CDCl$_3$ solutions. Chemical shifts δ are given in ppm with internal ^{1}H-TMS. Conductivity titrations were caried out at $T = 293$ K in acetonitrile solutions with a WTF LF-91 conductivity meter.

Synthesis and Crystallization of the Compounds. Complexes $[(NMBZT)I_2]$ (1) and $[\{(MBZIM)I_2\}\cdot\{(MBZIM)_2\cdot I^+\cdot I_3^-\}]$ (3) were prepared by mixing dichloromethane solutions of iodine with a suspension of the appropriate thione in dichloromethane solutions in molar ratios of 1:1 or 2:1 (L:I$_2$), in air, at 0 °C, with continuous stirring for 24 h. The mixtures were then filtered, and the resulting clear solutions were kept in the refrigerator for several days. Dark crystals of the complexes suitable for single-crystal analysis by X-ray crystallography were then grown and isolated by filtration. The reactions were also carried out in H$_2$O. The insoluble dark brown powders obtained were recrystallized from dichloromethane to yield the same products as previously.

Complex 1. Mw: 435.070. Mp: 90−92 °C. Anal. Found: C, 23.48; H, 1.61; N, 3.74; S, 14.86. Calcd for C$_8$H$_7$I$_2$NS$_2$: C, 22.09; H, 1.62; N, 3.22; S, 14.74. UV/vis (CH$_2$Cl$_2$): λ_{max} (log ϵ) = 476 nm (1.98), 326 nm (3.67), 240 nm (3.37). ^{1}H NMR (CDCl$_3$): δ = 7.62−7.34 {m, 4H, aromatic}, 3.90 [s, 3H, methylic] ppm.

Complex 3. Mw: 1211.990. Mp: 145−150 °C. Anal. Found: C, 21.16; H, 1.25; N, 7.26; S, 7.96. Calcd for C$_{21}$H$_{18}$I$_6$N$_6$S$_3$: C, 20.86; H, 1.25; N, 6.95; S, 7.96. UV/vis (CH$_2$Cl$_2$): λ_{max} (log ϵ) =

496 nm (3.02), 310 nm (5.05), 251 nm (4.46), 224 nm (4.87). ^{1}H NMR (CDCl$_3$): $\delta = 7.40-7.28$ [m, 4 H, aromatic] ppm.

Complex $\{[(NMBZT)_2I^+]\cdot[FeCl_4]^-$ **(2)** was prepared by adding 0.5 mmol of FeCl$_3$·6H$_2$O and 1.5 mmol of the thione ligand (*N*-methyl-2-mercaptobenzothiazole) to a 30 mL iodine solution (0.1 M) in dichloromethane in molar ratios of 1:3:6 (Fe^{3+}:L:I$_2$), in air, with continuous stirring for 4 h. The mixture was then filtered, and the resulting clear solution was kept for several days, at room temperature. Two types of small greenish black and thin pinlike shaped brown crystals were isolated. The greenish black ones were suitable for analysis by X-ray crystallography and proven to contain this compound. The pinlike crystals corresponded to the $\{[(NMBZT)_2I^+]\cdot[I_7]^-$ **(2a)** compound, with a known structure.[7a]

Complex 2. Mw: 813.995. Anal. Found: C, 20.55; H, 1.83; N, 3.30; S, 15.43. Calcd for C$_{16}$H$_{14}$Cl$_4$FeIN$_2$S$_4$: C, 20.61; H, 1.73; N, 3.44; S, 15.75. IR (cm^{-1}): 3449 m, 1655 w, 1460 s, 1426 s, 1370 vs, 1317 m, 1265 m, 1138 w, 1089 s, 1060 w, 981 s, 752 s, 631 m, 534 s. Far-IR (cm^{-1}): 280 m, 255 m, 160 m, 145 m, 125 m, 93 s, 79 s. UV/vis (CH$_2$Cl$_2$): λ_{max} (log ϵ) = 476 nm (1.98), 326 (3.67), 240 (3.37). Thermal analysis (% mass lost): 59.4 (I$_2$), 30.4 (thione).

Computational Details. The theoretical calculations have been performed using the Hartree–Fock (HF) quantum mechanical approach[20a] and density functional theory techniques (DFT).[20b] Because of the large number of electrons involved in the present systems, full geometry optimizations have been carried out only using DFT methodologies and, in particular, the B3LYP level of theory[20c,d] in combination with the LANL2DZ basis set.[20e,g] The HF approach combined with the same basis set was used for single-point energy computations at the B3LYP-optimized geometries.

All calculations have been performed with the Gaussian 98 series of programs.[21]

Crystal Data. Data were collected by the ω-scan technique in the $\theta-2\theta$ range 3.2–24.0° for **1** and 2.9–27.1° for **3** on a KUMA KM4CCD four-circle diffractometer,[22a] using graphite-monochromated Mo Kα ($\lambda = 0.710\ 73$ Å). Data for **2** were collected at 223 K on a Bruker SMART CCD diffractometer, also with Mo Kα radiation, so that $\theta_{max} = 30.0°$. Cell parameters were determined by a least-squares fit.[22b] All data were corrected for Lorentz–polarization effects and absorption..[22b] The structures were solved by direct-methods with SHELXS-97[23] and refined by full-matrix least-squares procedures on F^2. All non-hydrogen atoms were

refined anisotropically, and hydrogen atoms were located at calculated positions and refined as a ''riding model'' with isotropic thermal parameters fixed at 1.2× the U_{eq}'s of the appropriate carrier atom. During the refinement of **3**, it was noted that one of the two independent I$_3^-$ anions comprising the asymmetric unit was disordered about a center of inversion. Three atoms were included in the model, each assigned a site occupancy factor = 0.5. Symmetry expansion of this anion leads to a chain of iodide atoms (of half-weight) running parallel to the *b*-axis. The absolute structure of **1** was confirmed on the basis of the near zero value for the Flack parameter.

Reports CCDC-252519 (**1**), -253655 (**2**), and -252518 (**3**) contain the supplementary crystallographic data for this paper. These data can be obtained free of charge at www.ccdc.cam.ac.uk/conts/retrieving.html [or from the Cambridge Crystallographic Data Centre, 12 Union Road, Cambridge CB2 1EZ, U.K.; fax (internat.) +44-1223/336-033; e-mail deposit@ccdc.cam.ac.uk].

Supporting Information Available: Crystallographic data in CIF format. This material is available free of charge via the Internet at http://pubs.acs.org.

IC0484396

(20) (a) Hehre, W. J.; Radom, L.; Schleyer, P.v. R.; Pople, J. A. *Ab Initio Molecular Orbital Theory*; J. Wiley: New York, 1986. (b) Parr, R. G.; Yang, W. *Density Functional Theory of Atoms and Molecules*; Oxford University Press: Oxford, U.K., 1989. (c) Becke, A. D. *J. Chem. Phys.* **1993**, *98*, 5648–5652. (d) Lee, C.; Yang, W.; Parr, R. G. *Phys. Rev. B* **1988**, *37*, 785–793. (e) Wadt, W. R.; Hay, P. J. *J. Chem. Phys.* **1985**, *82*, 284–298. (f) Foresman, J. B.; Frish, A. *Exploring Chemistry with Electronic Structure Methods*; Gaussian Inc.: Pittsburgh, PA, 1995. (g) Russo, N.; Marino, T.; Sicilia, E.; Toscano, M. *Computational Methods in Sciences and Engineering*; Simos, T. E., Ed.; World Scientific: River Edge, NJ, 2003.

(21) Frisch, M. J.; Trucks, G. W.; Schlegel, H. B.; Scuseria, G. E.; Robb, M. A.; Cheeseman, J. R.; Zakrzewski, V. G.; Montgomery, J. A. Jr.; Stratmann, R. E.; Burant, J. C.; Dapprich, S.; Millam, J. M.; Daniels, A. D.; Kudin, K. N.; Strain, M. C.; Farkas, O.; Tomasi, J.; Barone, V.; Cossi, M.; Cammi, R.; Mennucci, B.; Pomelli, C.; Adamo, C.; Clifford, S.; Ochterski, J.; Petersson, G. A.; Ayala, P. Y.; Cui, Q.; Morokuma, K.; Malick, D. K.; Rabuck, A. D.; Raghavachari, K.; Foresman, J. B.; Cioslowski, J.; Ortiz, J. V.; Stefanov, B. B.; Liu, G.; Liashenko, A.; Piskorz, P.; Komaromi, I.; Gomperts, R.; Martin, R. L.; Fox, D. J.; Keith, T.; Al-Laham, M. A.; Peng, C. Y.; Nanayakkara, A.; Gonzalez, C.; Challacombe, M.; Gill, P. M. W.; Johnson, B.; Chen, W.; Wong, M. W.; Andres, J. L.; Head-Gordon, M.; Replogle, E. S.; Pople, J. A. *GAUSSIAN 98*; Gaussian, Inc.: Pittsburgh, PA, 1998.

(22) (a) *KUMA KM-4CCD user manual*; KUMA Diffraction: Wroclaw, Poland, 1999. (b) *CrysAlis, for reduction of the data from KUMA CCD diffractometer*; KUMA Diffraction: Wroclaw, Poland, 1999.

(23) Sheldrick, G. M. *SHELXS-97 (release 97-2) for crystal structure analysis and SHELXL-93 for refinement of crystal structure*; Institut fur Anorganische Chemie, University of Goettingen: Goettingen, Germany.